A bipotential organoid model of respiratory epithelium recapitulates high infectivity of SARS-CoV-2 Omicron variant

SUPPLEMENTARY INFORMATION

Supplementary Fig. S1. Cell populations in lung organoids.

Lung organoids were applied to flow cytometry to examine the percentage of airway and alveolar epithelial cell types. (a) Representative histograms of the cell-type markers. (b) Data represent the means ± SD of duplicated organoid samples from one donor.

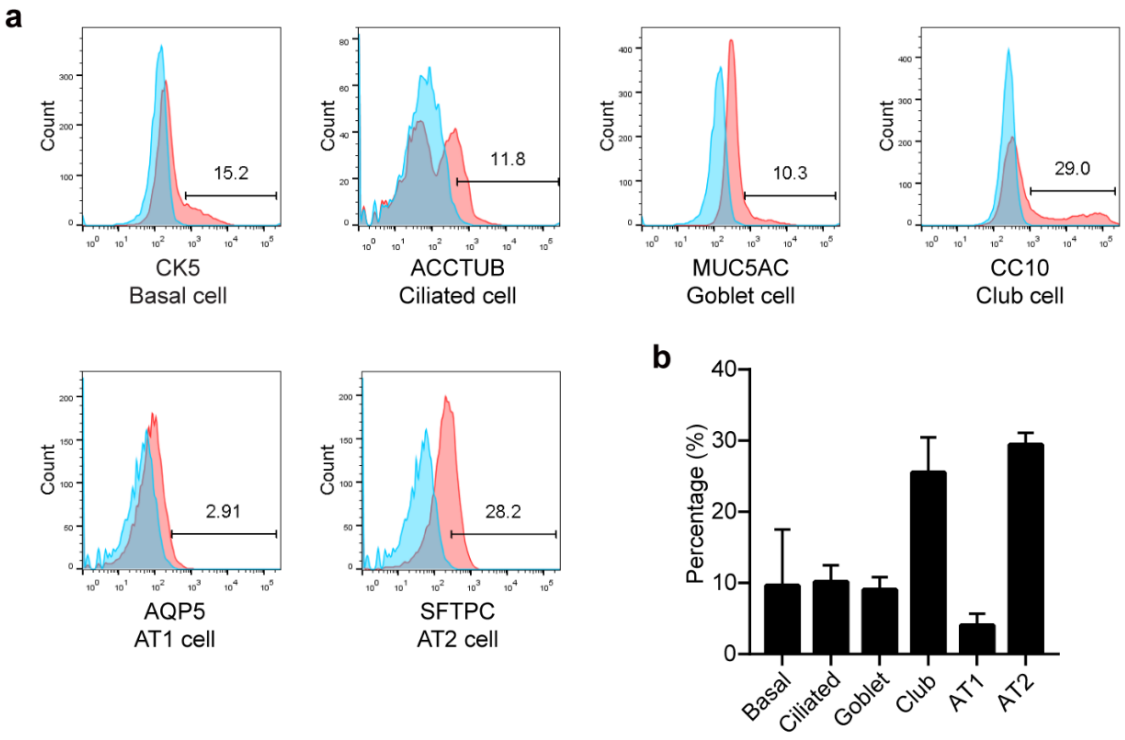

Supplementary Fig. S2. Marker gene expression in lung organoids during long-term culture.

Normalized expression levels of airway and alveolar cellular markers in expanding lung organoids were measured over the indicated time course. Data represent the means ± SD of duplicated organoid samples from one donor.

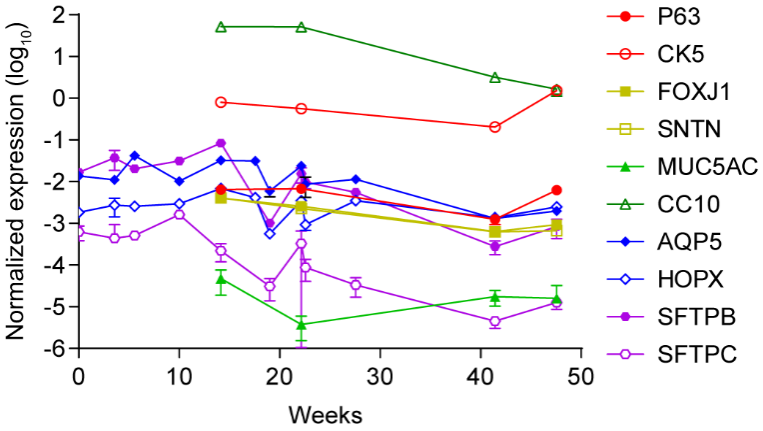

Supplementary Fig. S3. Reproducible alveolar differentiation in two lines of lung organoids.

Normalized expression levels of AT1- and AT2-cell markers were assessed in parental lung organoids (LO) from two different donors (a, b) and their derived alveolar organoids (AlvO). Data represent the means ± SD of a representative experiment in each organoid line, $n = 2$. Two-tailed unpaired Student's t-test.

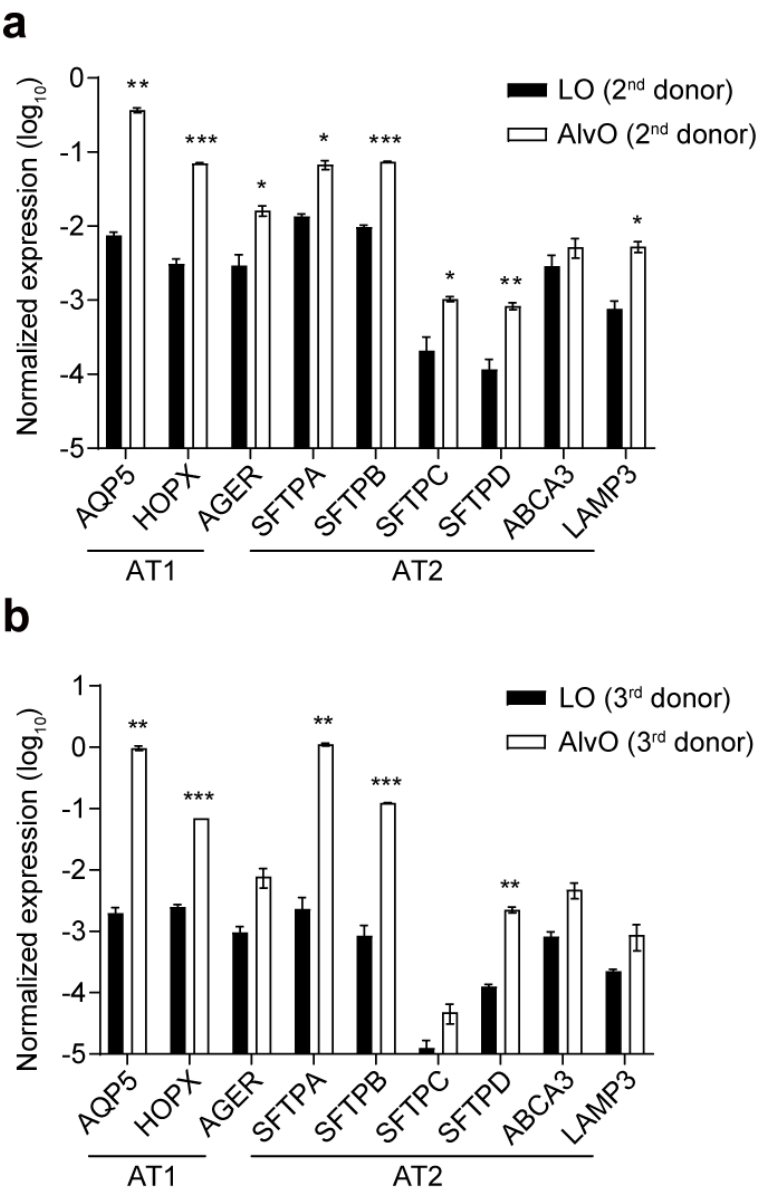

Supplementary Fig. S4. Suspension culture is required to induce alveolar differentiation.

Lung organoids were maintained in Matrigel overlaid with the expansion medium (black) or single cells suspension-cultured in DD medium (grey) or single cells embedded in Matrigel overlaid with DD medium (white) for 2 weeks. (a) Photomicrographs present the organoid morphology of day 14 after single cells were suspension-cultured in DD medium or embedded in Matrigel overlaid with DD medium. Scale bar, 100 μm. (b) The RT-PCR results show normalized expression levels of AT1- and AT2-cell markers. Data represent the means ± SD of a representative experiment, $n = 2$. Two-tailed unpaired Student's t-test.

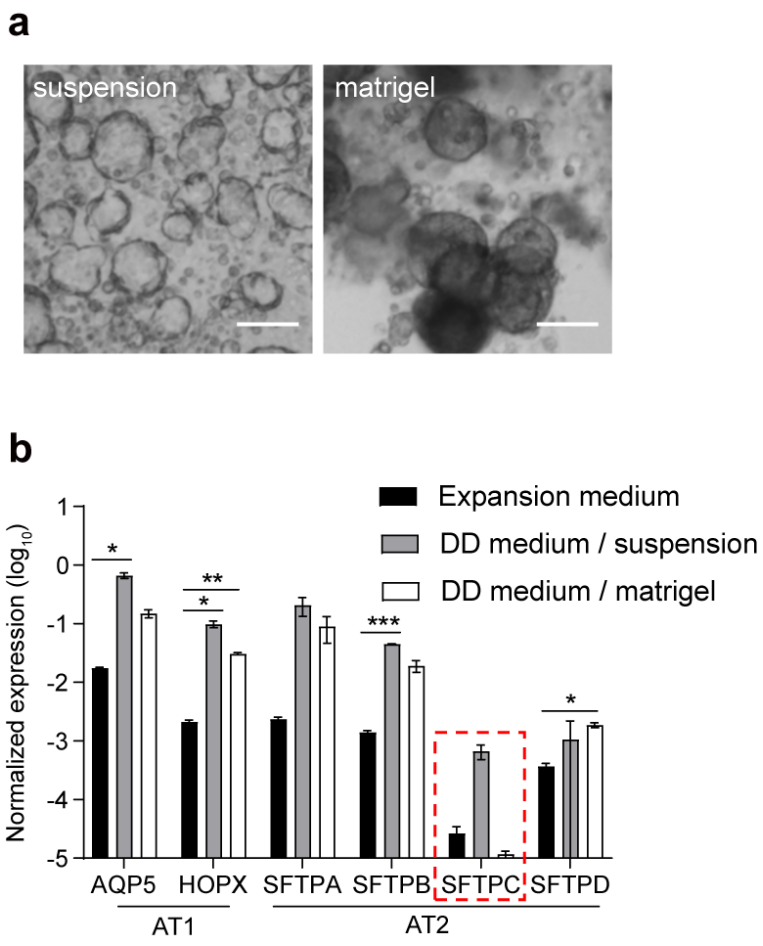

Supplementary Fig. S5. A WNT agonist induces alveolar differentiation.

Lung organoids were 3D cultured in the expansion medium (black) or suspension-cultured with DD medium supplemented with either Wnt3a conditioned medium (grey) or CHIR99021 (white) for 2 weeks and then applied to RT-qPCR assay. The results show normalized expression levels of AT1- and AT2-cell markers. Data represent the means ± SD of a representative experiment, $n = 3$. Two-tailed unpaired Student's t-test.

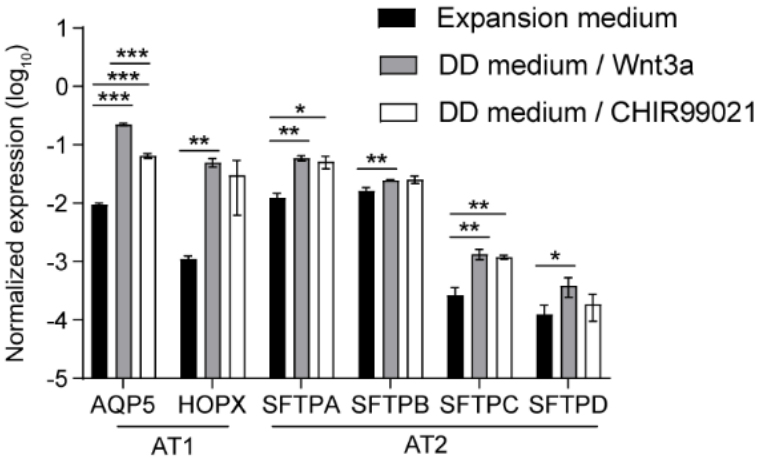

Supplementary Fig. S6. Reproducible derivation of alveolar organoids from lung organoids during 6 consecutive passages.

Normalized expression levels of AT1- (AQP5, HOPX) and AT2- (SFTPA, SFTPB, SFTPC, SFTPD) cell markers were assessed pairwise in lung organoids (LO) from one donor and the derived alveolar organoids (AlvO) during six consecutive passages. Data represent the means ± SD of an experiment, $n = 2$. Two-tailed unpaired Student's t-test.

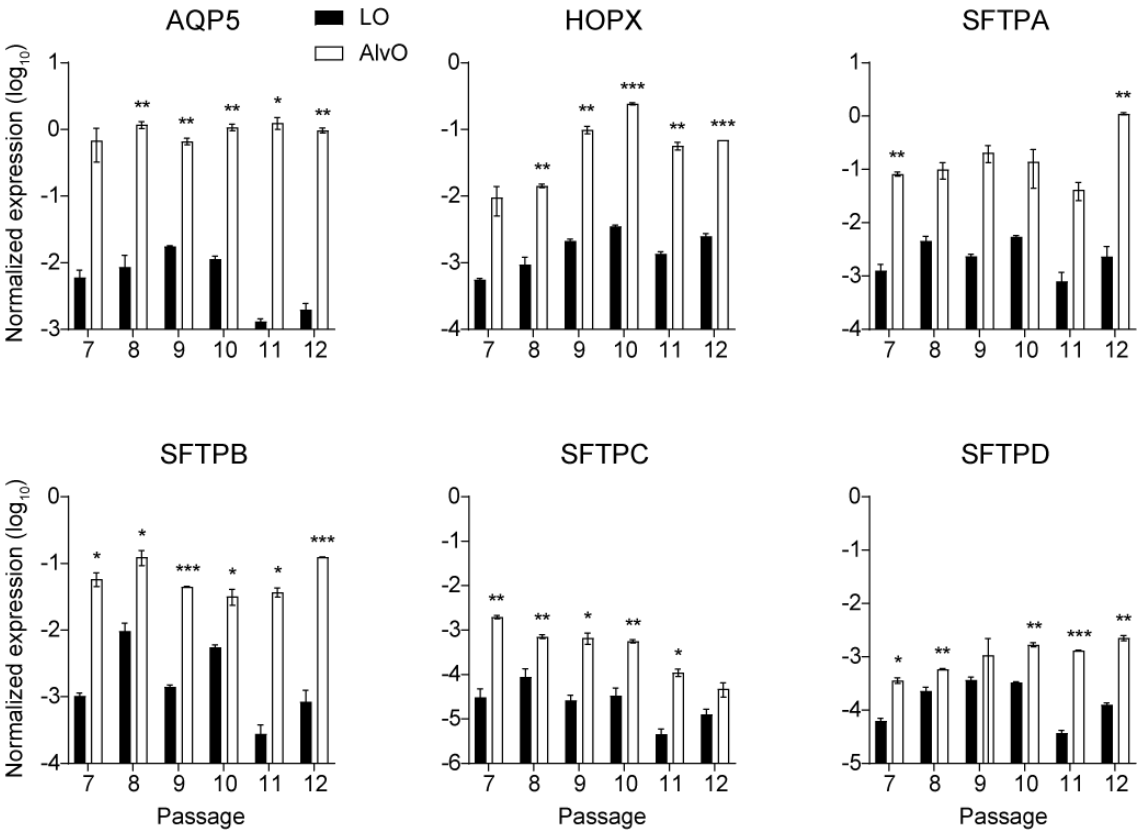

Supplementary Fig. S7. Higher abundance of cell-type proteins in alveolar organoids.

Parental LOs and differentiated AlvOs were applied to flow cytometry to examine the percentage (shown in Fig. 1D) and the intensity of AQP5$^+$ AT1 and SFTPC$^+$/LysoTracker red$^+$/HTII-280$^+$ AT2 cells. Data represent the means ± SD of the mean fluorescent intensity (MFI) of the positive cells in a representative experiment in one organoid line, n = 3 for AQP5 and SFTPC, n = 2 for LysoTracker red and HTII-280. Two-tailed unpaired Student's t-test.

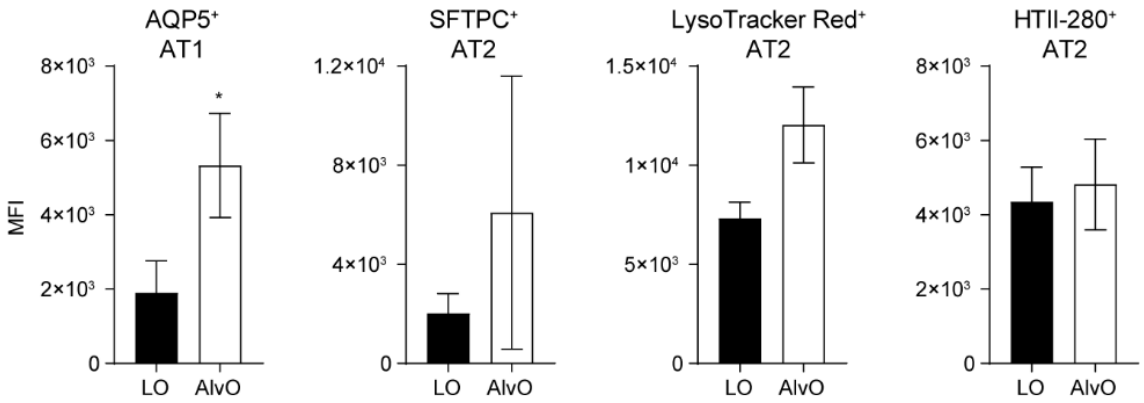

Supplementary Fig. S8. Staining and gating strategy for sorting AT2 cells in lung organoids.

(a) Top, histograms show the fluorescent signals of LysoTracker red (left, PE) and HTII-280 (right, FITC) of the stained lung organoids gated by isotype controls. Red, cells stained with the dye or the specific antibody; blue, cells mock-stained or stained with an isotype control. Bottom, dot plots show the stepwise gating of the single-cell suspension from lung organoids. (b) Lung organoids derived from sorted AT2 cells (AT2-LO) were applied to flow cytometry to examine the percentage of airway and alveolar epithelial cell types. Representative histograms of the cell-type markers were shown.

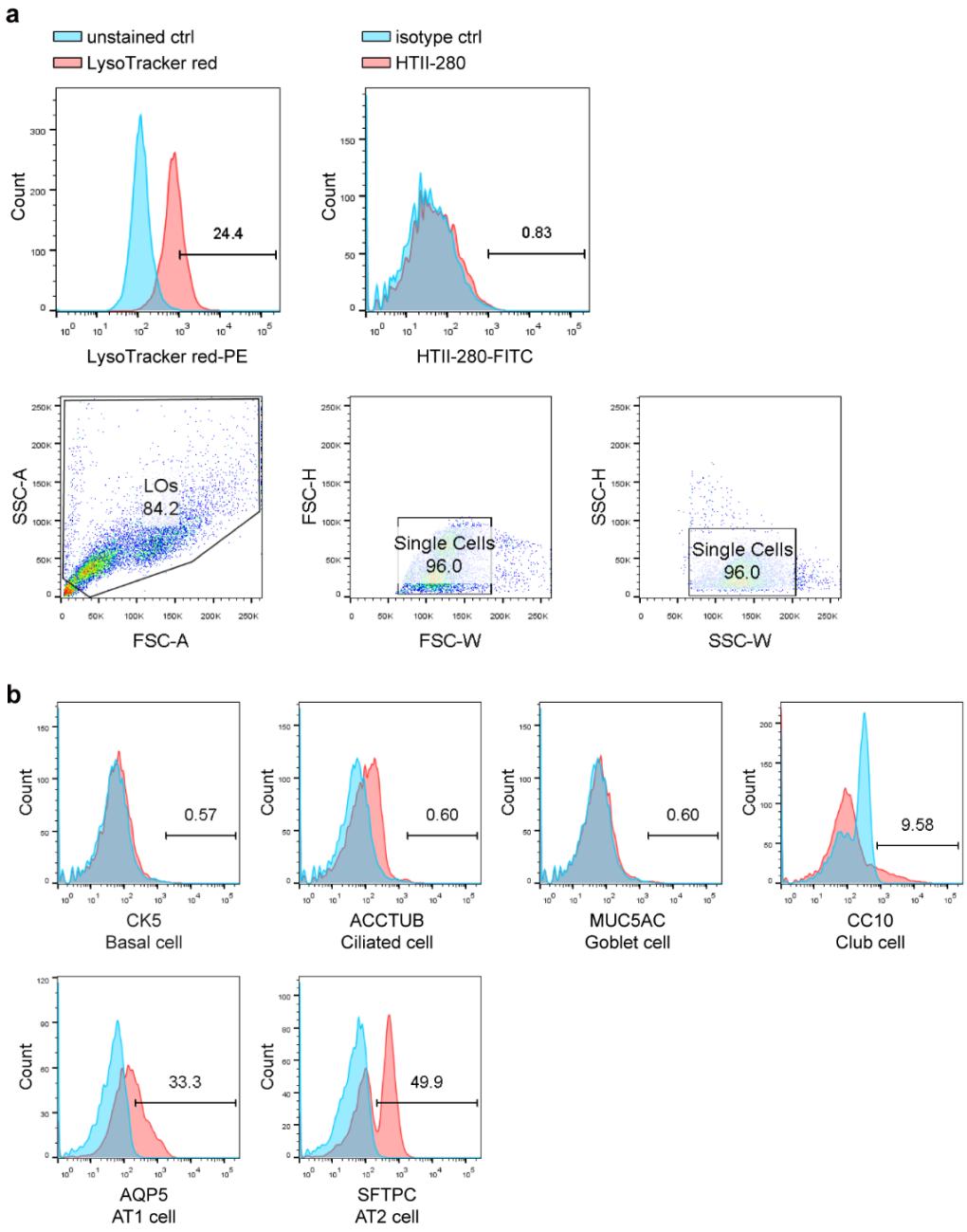

Supplementary Fig. S9. ACE2 expression in ciliated cells and AT2 cells.

ACE2 and TMPRSS2 expression in airway organoids (3D AwO & 2D AwO) and alveolar organoids (AlvO) differentiated from the same organoid line were detected by flow cytometry. Representative dot plots show the AwOs co-stained with ACCTUB (PE-Texas red) and ACE2 (FITC), and the AlvOs co-stained with SFTPC (PE-Texas red) and ACE2 (FITC). Red, cells stained with specific antibodies; blue, cells stained with isotype controls.

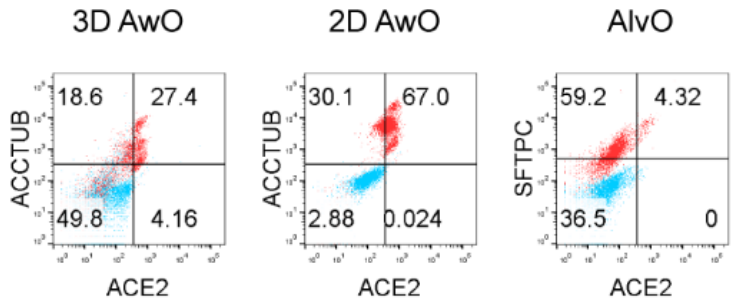

Supplementary Fig. S10. Increased ciliated cell population and ACE2 expression in 2D airway organoids cultured in slightly acidic medium.

Flow cytometry was performed to analyze the percentages of (a) ACCTUB^{+} ciliated cells, (b) ACE2^{+} and TMPRSS2^{+} cells in the 2D AwOs differentiated in pH 6.6/7.4 or 7.4/7.4. Data represent the means ± SD of a representative experiment, *n* = 4 (ACCTUB) or *n* = 2 (ACE2/TMPRSS2) respectively. Two-tailed unpaired Student's t-test.

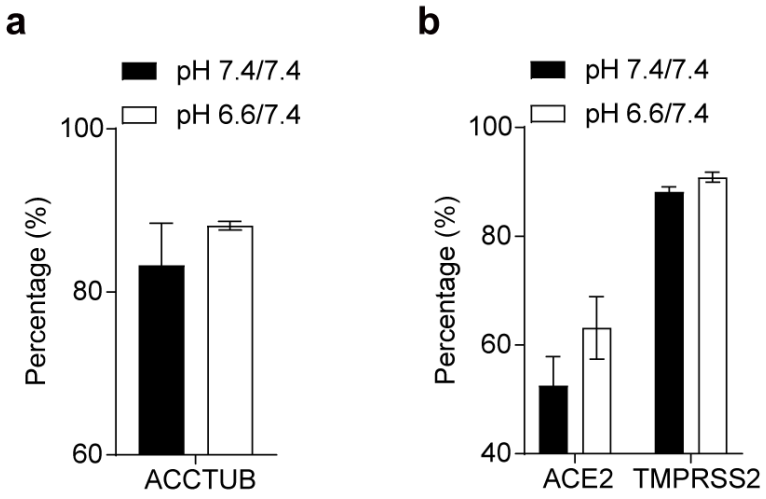

Supplementary Fig. S11. Replicative fitness of SARS-CoV-2 variants in Vero E6/TMPRSS2 cells.

At the indicated hours after inoculation with wildtype (WT) or the Omicron variant (MOI = 0.01), culture media were harvested from the VeroE6/TMPRSS2 cells and applied to viral load detection and viral titration by TCID50 assay. Data show means ± SD of a representative experiment, *n* = 3. Two-tailed unpaired Student's t-test.

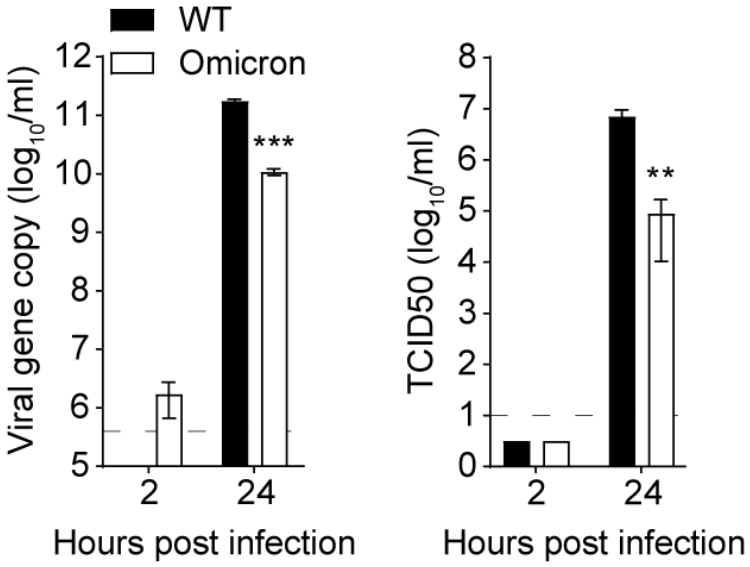

Supplementary Table S1. qPCR Primer list.

Gene	Sequence	
SARS-CoV-2 RdRp	F	CGCATACAGTCTTRCAGGCT
	R	GTGTGATGTTGAWATGACATGGTC
	Probe	FAM-TTAAGATGTGGTGCTTGCATACGTAGAC-lABkFQ
AQP5	F	GCTCACTGGGTTTTCTGGGTA
	R	TCCATGGTCTTCTTCCGCTC
HOPX	F	GCCTTTCCGAGGAGGAGAC
	R	TCTGTGACGGATCTGCACTC
AGER	F	GTGTCCTTCCCAACGGCTC
	R	ATTGCCTGGCACCGGAAAA
SFTPA	F	GATGGGCAGTGGAATGACAGG
	R	GGAATGAAGTGGCTAAGGGT
SFTPB	F	GCAGACGTCCATAGCTCCTC
	R	AGGGACACTTCCAGGCATTT
SFTPC	F	AGCAAAGAGGTCCTGATGGA
	R	CGATAAGAAGGCGTTTCAGG
SFTPD	F	TGGGCTTCCAGATGTTGCTT
	R	CGACACTTTGGCCATTTGGG
ABCA3	F	AGATGTAGCGGACGAGAGGA
	R	GCTGCTCGTACACCTTGGAG
LAMP3	F	AAGATGACCACTTTGGAAATGTG
	R	GATGGCCCCAATCACAGGAA
P63	F	CAGACTCAATTTAGTGAGCC
	R	CTGCTGGTCCATGCTGTT
CK5	F	GAGGAATGCAGACTCAGTGGA
	R	TAGCTTCCACTGCTACCTCCG
FOXJ1	F	TCGTATGCCACGCTCATCTG
	R	CGGATTGAATTCTGCCAGGT
SNTN	F	GCTGCAAACCCAATTTAGGA
	R	TGCTCATCAAGTTCAGAAAGGA
MUC5AC	F	CCTACAAAGCTGAGGCCTGT
	R	GACCCTCCTCTCAATGGTGC
CC10	F	AGCATCATTAAGCTCATGGAAAAA
	R	GTGGACTCAAAGCATGGCAG
GAPDH	F	GGAGCGAGATCCCTCCAAAAT
	R	GGCTGTTGTCATACTTCTCATGG

Supplementary Table S2. Antibody list.

Name	Supplier	Cat. no.	Lot no.	Dilution (IF)	Dilution (Flow)
Mouse IgG1	abcam	ab91353	GR3327311-3	-	1:100
Mouse IgM	abcam	ab18401	GR3336129-2	-	1:100
Rabbit IgG	abcam	ab172730	GR3284310-8	-	1:100
Goat IgG	R&D systems	AB-108-C	ES4120071	-	1:100
Rat IgG	invitrogen	10700	RA226537	-	1:100
ACE2	R&D systems	AF933	HOK0620051	1:100	1:100
TMPRSS2	invitrogen	PA5-14264	SI2433683G	-	1:100
AQP5	abcam	ab92320	GR97210-39	1:100	1:100
SPB	Santa Cruz Biotech	sc-133143	D2418	1:50	-
pro-SPC	Sigma-Aldrich	AB3786	3041829	-	1:100
HTII-280	Terrace Biotech	TB-27AHT2-280	KM27	1:100	1:100
P63	abcam	ab124762	GR303296-1	1:100	-
CK5	abcam	ab128190	GR239416-18	-	1:100
FOXJ1	Sigma-Aldrich	HPA005714	G114396	1:50	-
TUBULIN	abcam	ab179509	GR252919-6	-	1:1000
TUBULIN	Sigma-Aldrich	T7941	088M4793	1:100	1:1000
CC10	R&D systems	MAB4218	YWN0218091	-	1:100
MUC5AC	abcam	ab3649	GR126783	-	1:1000
SARS-CoV-2 NP	in-house	-	-	1:1000	-
J2 (dsRNA)	Scicons	10010500	17741	-	1:100
Goat anti-Mouse 488	invitrogen	A-11001	2090562	1:500	1:500
Goat anti-Mouse 594	invitrogen	A-11005	1750828	1:500	-
Goat anti-Rabbit 488	invitrogen	A-11034	1885241	1:500	1:500
Goat anti-Rabbit 594	invitrogen	A-11037	1608397	1:500	-
Donkey anti-Goat 488	invitrogen	A-11055	1771339	1:500	1:500
Donkey anti-Rat 488	invitrogen	A-21208	1900239	-	1:500
Goat anti-Guinea pig 488	invitrogen	A-11073	1990462	1:500	-